# Influences of the change of neutron number on the charge form factors of Ca and Ni isotopes*

WANG Zai-Jun(王再军)[1;1)] REN Zhong-Zhou(任中洲)[2,3]

1 (Department of Mathematics, Physics and Information Science, Tianjin University of Technology and Education, Tianjin 300222, China)
2 (Department of Physics, Nanjing University, Nanjing 210008, Chain)
3 (Center of Theoretical Nuclear Physics, National Laboratory of Heavy-Ion Accelerator at Lanzhou, Lanzhou 730000, China)

**Abstract** We calculate the charge form factors of the even-even isotopes on the $Z$=20 and 28 isotopic chains, including both the stable nuclei and unstable ones, and investigate the influences of the change of neutron number on the charge form factors of the Ca and Ni isotopes systematically with the relativistic eikonal approximation associated with the self-consistent relativistic mean field model. We find that the charge form factor changes significantly and regularly with the variation of neutron number. The charge form factors shift outward and downward as the nucleus moves from the very neutron-rich region to the very proton-rich region along an isotopic chain. The significant shift shows that the charge form factor is very sensitive to a change of neutron number. The regularity of the variation of the charge form factors along an isotope chain may suggest certain laws which rules the influence of the neutrons on the distribution of the protons. The calculations will provide a useful reference for the future experiments as well as a test of the reliability of the relativistic mean field model for unstable nuclei far from the stability line.

**Key words** Ca isotopes, Ni isotopes, elastic electron scattering, charge form factor, relativistic eikonal approximation

**PACS** 21.10.Ft, 25.30.Bf

## 1 Introduction

Our interest in studying the influences of the change of proton number on the charge form factors arises from the recent achievements in the research of nuclear physics[1—18] and from the research projects which will be performed on the new electron-RI beam colliders[19—22]. Although the charge form factors and cross sections for stable nuclei have been well investigated, studies on the charge form factors and cross sections for unstable nuclei far from the β-stability line are very rare. Many interesting questions relating to unstable nuclei remain to be solved. How are the nucleons distributed in an unstable nucleus far from the stability line? Do the firmly established properties, such as the magic number, for the stable nuclei still exist for the unstable ones? Do the nuclear models established based on the knowledge of stable nuclei still valid for the unstable nuclei? Clarification of all these questions will finally depend on our understanding of unstable nuclei. Therefor, it is of practical meaning to study the structure of unstable nuclei by electron scattering. In order to find out the sensitivity of the charge form factor to a change of the charge distribution, some calculations and discussions have been done in term of the model-dependent

Received 8 July 2008
* Supported by National Natural Science Foundation of China (10675090, 10125521, 10535010) and Start-up Fund of Tianjin University of Technology and Education for Scientific Research (KYQD05009)
1) E-mail: zaijunwang99@126.com

method in Ref. [20]. In our earlier work, we also did some exploratory calculations on the unstable nuclei $^{28}$S and $^{12}$O[23]. In the present paper, we will carry out a systematic calculation of the charge form factors for the even isotopes of Ca ($A$=34—60) and Ni ($A$=48—80) with the relativistic eikonal approximation within the framework of the relativistic mean field theory. Ca- and Ni-isotope chains are two typical isotopic chains with magic proton number in the medium-heavy region. Therefore, they will be the appropriate candidate nuclei for the future electron-nucleus scattering experiments. The main purpose of this paper is to give a full presentation of charge form factors for a typical isotopic chain and try to find out the influences of the change of proton number on the charge form factors on an isotopic chain. This will serve as a good reference for the future experiments.

This paper is organized in the following way. Section 2 is the formalism of the relativistic eikonal approximation for electron scattering and a brief review of the RMF model. The numerical results and discussions are presented in Sec. 3. A summary is given in Sec. 4.

## 2 Formalism

### 2.1 The relativistic eikonal approximation

The starting point of the relativistic eikonal approximation is the Dirac equation for a particle moving in a scalar potential $V(\boldsymbol{r})$[24, 25],

$$(\alpha\cdot\boldsymbol{p}+\beta m-E)\psi(\boldsymbol{r})=-V(\boldsymbol{r})\psi(\boldsymbol{r}), \tag{1}$$

where $E$ and $m$ are energy and mass of the incident particle, respectively, and $\alpha$ and $\beta$ are the Dirac matrices. Using Green's function method, the scattering amplitude can be expressed in the following form[25]:

$$f(\theta)=-\frac{1}{4\pi}(\alpha\cdot\boldsymbol{k_f}+\beta m+E)\int \mathrm{e}^{-\mathrm{i}\boldsymbol{k_f}\cdot\boldsymbol{r}}V(\boldsymbol{r})\psi(\boldsymbol{r})\mathrm{d}\boldsymbol{r}, \tag{2}$$

where $\theta$ is the scattering angle, and $\boldsymbol{k_f}$ is the outgoing momentum.

Under high-energy approximation, the elastic differential cross section $\sigma$ and form factor $F(q)$ can be expressed as[25]:

$$\sigma=\cos^2\left(\frac{1}{2}\theta\right)|I_1(q)+I_2(q)|^2\ , \tag{3}$$

and

$$|F(q)|^2=\frac{\sigma}{\sigma_{\mathrm{M}}}, \tag{4}$$

where $q$ is the momentum transfer, $\sigma_{\mathrm{M}}$ is the Mott cross section. $I_1(q)$ and $I_2(q)$ are given by the following integrals:

$$I_1(q) = -\mathrm{i}k\int_0^R J_0(qb)[\mathrm{e}^{2\mathrm{i}\chi(b)}-1]b\,\mathrm{d}b, \tag{5}$$

$$I_2(q) = -\mathrm{i}k\int_R^\infty J_0(qb)[\mathrm{e}^{2\mathrm{i}\chi(b)}-1]b\,\mathrm{d}b, \tag{6}$$

where $b$ is the impact parameter, $R$ is the cutoff cylindrical radius, $k=|\boldsymbol{k}_0|$, and $J_0$ is the Bessel function. For high energy electrons ($E\approx k$), $\chi(b)$ can be written as[24, 25]:

$$\chi(b)=-\frac{1}{2}\int_{-\infty}^{\infty}V(r)\,\mathrm{d}z, \tag{7}$$

$$r=\sqrt{b^2+z^2}. \tag{8}$$

The earlier Eqs. (1)—(8) along with the Coulomb attraction correction and the target nucleus recoil effect correction[23] enable us to calculate the form factors for a given charge density distribution.

### 2.2 The relativistic mean-field model

Since the RMF model is a standard theory and the details can be found in many works[26—30], we only give the main elements here. The starting point of this model is an effective Lagrange density $\mathcal{L}$ for the interacting nucleons, the σ, ω, ρ mesons, and photons,

$$\begin{aligned}\mathcal{L} = {}& \bar{\Psi}(\mathrm{i}\gamma^\mu\partial_\mu-m)\Psi-g_\sigma\bar{\Psi}\sigma\Psi-g_\omega\bar{\Psi}\gamma^\mu\omega_\mu\Psi-\\ & g_\rho\bar{\Psi}\gamma^\mu\rho^{\mathrm{a}}_\mu\tau^{\mathrm{a}}\Psi+\frac{1}{2}\partial^\mu\sigma\,\partial_\mu\sigma-\frac{1}{2}m_\sigma^2\sigma^2-\frac{1}{3}g_2\sigma^3-\\ & \frac{1}{4}g_3\sigma^4-\frac{1}{4}\Omega^{\mu\nu}\Omega_{\mu\nu}+\frac{1}{2}m_\omega^2\omega^\mu\omega_\mu+\frac{1}{4}c_3(\omega_\mu\omega^\mu)^2-\\ & \frac{1}{4}R^{a\mu\nu}\cdot R^a_{\mu\nu}+\frac{1}{2}m_\rho^2\rho^{\mathrm{a}\mu}\cdot\rho^{\mathrm{a}}_\mu-\frac{1}{4}F^{\mu\nu}F_{\mu\nu}-\\ & \mathrm{e}\bar{\Psi}\gamma^\mu A_\mu\frac{1}{2}(1-\tau^3)\Psi,\end{aligned} \tag{9}$$

with

$$\Omega^{\mu\nu} = \partial^\mu\omega^\nu-\partial^\nu\omega^\mu, \tag{10}$$

$$R^{\mathrm{a}\mu\nu} = \partial^\mu\rho^{\mathrm{a}\nu}-\partial^\nu\rho^{\mathrm{a}\mu}, \tag{11}$$

$$F^{\mu\nu} = \partial^\mu\ A^\nu-\partial^\nu\ A^\mu, \tag{12}$$

where the meson fields are denoted by $\sigma$, $\omega_\mu$, and $\rho^{\mathrm{a}}_\mu$ and their masses are denoted by $m_\sigma$, $m_\omega$, and $m_\rho$, respectively. The nucleon field and rest mass are denoted by $\Psi$ and $m$. $A_\mu$ is the photon field

which is responsible for the electromagnetic interaction, $\alpha = 1/137$. The effective strengths of the coupling between the mesons and nucleons are, respectively, $g_\sigma$, $g_\omega$, and $g_\rho$. $g_2$ and $g_3$ are the nonlinear coupling strengths of the σ meson. $c_3$ is the self-coupling term of the ω field. The isospin Pauli matrices are written as $\tau^a$, $\tau^3$ being the third component of $\tau^a$.

Under the no-sea approximations and mean-field approximations, a set of coupled equations for mesons and nucleons can be easily obtained by the variational principle[31—34]. This set of equations can be solved consistently by iterations. After a final solution is obtained, we can calculate the binding energies, root-mean-square radii of proton, and neutron density distributions, single particle levels. The details of numerical calculations are described in Refs. [31, 32].

## 3 Numerical results and discussions

### 3.1 Variation of charge densities and charge form factors for Ca isotopic chain

We first produce the charge densities for the even Ca isotopes $^{34—60}$Ca with the RMF model. In the calculation, the NL-SH force parameters[35] are used. The pairing gaps for open shell nuclei are included by the Bardeen-Cooper-Schrieffer (BCS) treatment. The standard input for pairing gaps are $\Delta_n = \Delta_p = 11.2/\sqrt{A}$ MeV. For the very neutron-rich nuclei, we assume that the last neutrons just occupy the bound levels according to Tanihata[36, 37]. The main results of the RMF model are presented in Figs. 1—3.

Figure 1 is the total binding energies for even Ca isotopes. The filled and empty squares correspond to the theoretical results and experimental ones[38] respectively. It is seen that the calculated binding energies agree with the experimental results very well.

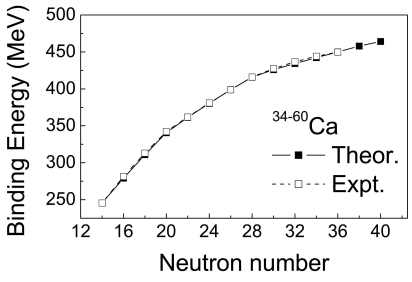


Fig. 1. The total binding energies for the even isotopes of Ca ($A$=34—60).

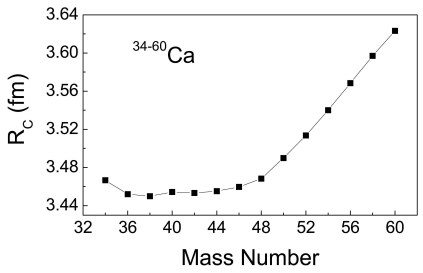


Fig. 2. The calculated root-mean-square charge radii for the even isotopes of Ca ($A$= 34—60) by the RMF model.

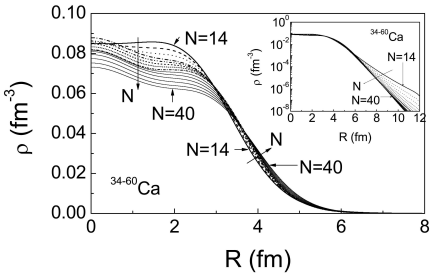


Fig. 3. The charge density variation with neutron number from the RMF model for the even isotopes of Ca ($A$=34—60). The arrow points to the direction in which the neutron number increases.

Figure 2 shows the calculated root-mean-square (rms) charge radii of $^{34-60}$Ca. The RMF results for $^{40}$Ca and $^{48}$Ca are respectively 3.454 fm and 3.468 fm. The experimental rms charge radius is 3.450 fm for $^{40}$Ca and 3.451 fm for $^{48}$Ca[39]. The deviation between the theoretical rms charge radii and the experimental ones is less than 0.02 fm. The smallest charge radii fall to the stable isotopes near or on the stability line. The charge radius becomes larger as the isotope falls far from the stability line. This indicates that the number of neutrons has significant influences on the charge size and charge distribution. In order to show these influences clearly, we plot the charge densities in Fig. 3. One can find from this figure that the charge distribution varies considerably from isotope to isotope. The variation of the charge densities for different isotopes has the following features. First, the densities around the center of the nuclei ($r < 3$ fm) decrease as the neutron number increases. $^{60}$Ca has the smallest densities and $^{34}$Ca has the largest ones. Second, the surface of the charge density distribution becomes sharper when more neutrons are added to an isotope. And the third, the spatial extension of charge of the neutron-deficient isotopes is larger than that of the neutron-rich ones, although the latter has a larger rms charge radius. This can be seen clearly

from the inset (in logarithmic scale) in Fig. 3. Finally, it has been known that there exists shell effect in the charge distributions of $^{40,48}$Ca, since their proton numbers are a magic number and they have closed proton shells. But the two peaks, which embody the shell effect, in the charge density distribution tend to disappear as the number of neutrons decreases. This suggests that the shell effect of the charge distribution seems to disappear for the very neutron-deficient isotopes. All these features show that the isotope effect in nuclear charge distribution of Ca isotopes is pronounced. The extreme deficiency and extreme richness in neutrons may have considerable influences on the ground-state structure of nuclei. They may lead to very different charge distributions and level structures for unstable nuclei near the drip lines.

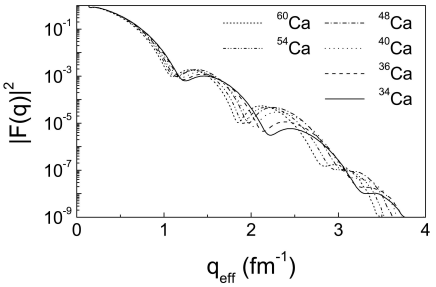


Fig. 4. The charge form factor variation with neutron number from the relativistic eikonal approximation for $^{34}$Ca, $^{36}$Ca, $^{40}$Ca, $^{48}$Ca, $^{54}$Ca, and $^{60}$Ca. The isotope effect in the charge form factors of Ca isotopes is clearly demonstrated.

Different charge density distributions will certainly lead to different charge form factors, since the latter is directly related to the former. Using the charge densities given in Fig. 3, we can make our predictions of charge form factor for Ca isotopes by the relativistic eikonal approximation. The charge form factors for $^{34}$Ca, $^{36}$Ca, $^{40}$Ca, $^{48}$Ca, $^{54}$Ca, and $^{60}$Ca are shown in Fig. 4. It is seen from this figure that there are two important aspect to which we shall pay attention. One is that the charge form factor varies appreciably from isotope to isotope. This suggests that the charge form factor is very sensitive to the changes of neutron number. Compared with the charge form factors of the stable isotopes, the charge form factors of the neutron-rich isotopes have a considerably large inward and upward shift and those of the neutron-deficient isotopes a significantly large outward and downward shift. The richer or more deficient the neutrons are in an isotope, the larger the shift of the charge form factor is. The shifts of minimums and maximums of the charge form factors suggest that the surface of the charge density distribution tends to become sharper when more and more neutrons are added. In the range of low-momentum transfer (q<1 fm$^{-1}$), the charge form factors tend to decrease in magnitude as the neutron number increases. This can be accounted for by the following relation between the charge form factor and the rms charge radius at low momentum transfers.

$$F(q) = 1 - \frac{1}{6}q^2\langle r^2\rangle + \cdots \ . \tag{13}$$

Therefore, in the range of low-momentum transfer, the decrease of the form factors in magnitude with the increase of the neutron number means that the rms charge radius tends to become larger as more neutrons are added. This is in agreement with the RMF results of the rms charge radii and of the charge densities shown in Figs. 2 and 3. The isotopic shifts of the rms charge radii can be determined, if the charge form factors at low momentum transfers are precisely measured. Charge form factors in the range of moderate- and high-momentum transfer are mainly related to the details of the charge density distribution. Therefore, the shape of the charge distribution can be determined by measuring the form factors in this region of momentum transfer. One can find that the minimums and maximums are very sensitive to the variation of neutron number. Hence, the charge form factors or the isotopic shifts of the charge form factor can be measured by electron-nucleus scattering experiments. With these data, the charge density can be extracted using the model-dependent method or the model-independent analysis (Fourier-Bessel series expansion). Another important aspect of variation of the charge form factors is the regular pattern of the isotopic shifts. This may suggest certain laws which rule the influence of neutrons on the distribution of protons. This problem deserves to be further studied.

### 3.2 Variation of charge densities and charge form factors for Ni isotopic chain

With the same method and procedure as we used in calculation for Ca isotopic chain, the total binding energies, rms charge radii, and the charge form factors for Ni isotopic chain can also be calculated. The results are presented in Figs. 5—8.

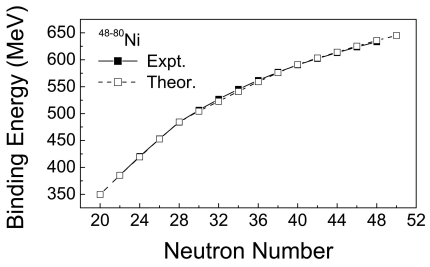


Fig. 5. The total binding energies for the even isotopes of Ni ($A$=48—80). The theoretical ones are calculated with RMF model. The experimental data are taken from Ref. [38].

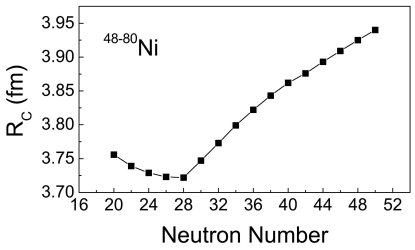


Fig. 6. The calculated root-mean-square charge radii for the even isotopes of Ni ($A$= 48—80) with the RMF model.

Figure 5 depicts the experimental total binding energies[38] and the calculated ones by the RMF model. The comparison shows very good agreement between the theoretical results and the experimental data. Fig. 6 represents the RMF results of the rms charge radii for the even isotopes of Ni. The figure shows that the stable isotopes have the smallest rms charge radii. The neutron-rich and neutron-deficient isotopes have a larger charge radius. The charge radius becomes even larger when more neutrons are added to or subtracted from a stable isotope. The experimental charge radius for the stable isotopes $^{58}$Ni, $^{60}$Ni, $^{62}$Ni, $^{64}$Ni are, respectively, 3.742 fm, 3.764 fm, 3.802 fm, and 3.821 fm [39]. The calculated results corresponding to the four isotopes are, 3.747 fm, 3.773 fm, 3.799 fm, and 3.822 fm respectively. The deviation between the theoretical rms charge radii and the experimental ones is less than 0.02 fm. In Fig. 7, we plot the charge densities for the even isotopes of Ni. The variation of charge density distributions with neutron number are similar to those of Ca isotopes apart from two exceptions. One is that the shell effect is more pronounced for Ni isotopes than for Ca isotopes. Another is that the shell effect tends to disappear for very neutron-deficient isotopes of Ca (see Fig. 4), but still exist for very neutron-deficient Ni isotopes. These two differences may be due to that $Z$=28 is a better proton shell closure than $Z$=20 although both $Z$=28 and $Z$=20 are shell closure. The $Z$=20 proton shell closure is more easily influenced by a change of neutron number than the $Z$=28 proton shell closure. Currently, some experimental researches have been done on this aspect, and it is shown that certain neutron magic numbers may disappear and some new neutron magic numbers may exist in the very neutron-rich region[15—18]. Perhaps, this phenomenon also exist for protons for the proton-rich nuclei near the proton-drip line.

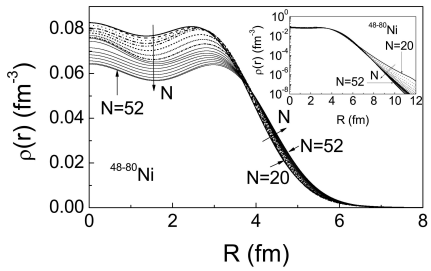


Fig. 7. The charge density variation with neutron number from the RMF model for the even isotopes of Ni ($A$=48—80). The inset is in logarithmic scale. The arrow points to the direction in which the neutron number increases.

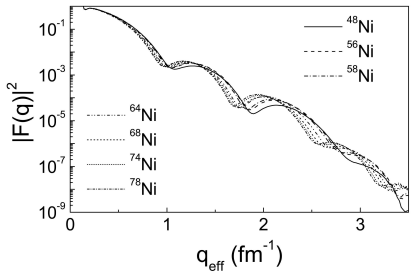


Fig. 8. The charge form factor variation with neutron number from the relativistic eikonal approximation for $^{48}$Ni, $^{56}$Ni, $^{58}$Ni, $^{64}$Ni, $^{68}$Ni, $^{74}$Ni, and $^{78}$Ni. The isotope effect in the charge form factors of Ni isotopes is clearly demonstrated.

Figure 8 shows the calculated charge form factors for $^{48}$Ni, $^{56}$Ni, $^{58}$Ni, $^{64}$Ni, $^{68}$Ni, $^{74}$Ni, and $^{78}$Ni isotopes. This figure gives a full description of the variation of charge form factors with neutron number for the even isotopes of Ni. It is seen that the variation of the charge form factor of Ni isotopes is very similar to that of Ca isotopes. When the neutron number changes, the charge form factors vary significantly and with a regular pattern. This suggests that the charge form factor is very sensitive to the changes of the neutron number. It is expected

that this isotope effect can be observed in the next-generation electron-RI beam collider. By accurately measuring the isotopic shifts of the charge form factor on an isotopic chain, the charge density distributions for the unstable nuclei can be determined.

## 4 Conclusion

In summary, we have performed a study of the influences of the change of neutron number on the charge form factors of Ca and Ni isotopes. Calculations for Ca and Ni isotopic chains show that the charge form factors vary significantly and with a regular pattern as the number of neutrons changes. The maximums and minimums of the charge form factor have a pronounced shift when the neutron number changes. The isotopic shifts of the charge form factors have observable effects. If the isotopic shifts of the charge form factor for unstable nuclei are precisely measured by the future electron scattering experiment, the charge size and the charge distribution can be determined. Thus it will be very interesting to measure the charge form factors on an isotopic chain by the electron-nucleus scattering experiment (at RIKEN[19, 20] and GSI[21, 22]). Our calculations will serve as a good reference for the coming experiments. Another important aspect of this paper is that our calculations will provide a further test of the reliability of the RMF model to unstable nuclei far from the β-stable line.

### References


1 Tanihata I. Prog. Part. Nucl. Phys., 1995, **35**: 505
2 Geissel H, ünzenberg G. M, Riisager K. Ann. Rev. Nucl. Part. Sci., 1995, **45**: 163
3 Mueller A. Prog. Part. Nucl. Phys., 2001, **46**: 359
4 ZHANG Hu-Yong, SHEN Wen-Qing, REN Zhong-Zhou et al. Nucl. Phys. A, 2002, **707**: 303
5 LI Zhi-Hong, LIU Wei-Ping, BAI Xi-Xiang et al. Phys. Lett. B, 2002, **527**: 50
6 REN Zhong-Zhou, XU Gong-Ou. Phys. Lett. B, 1990, **252**: 311
7 Bertsch G F, Esbensen H. Ann. Phys., 1991, **209**: 327
8 Zhukov M V, Danilin B V, Fedorov D V et al. Phys. Rep., 1993, **231**: 151
9 Hansen P G, Jensen A S, Jonson B. Ann. Rev. Nucl. Part. Sci., 1995, **45**: 591
10 Al-khalili J S, Tostevin J A, Thompson I J. Phys. Rev. C, 1996, **54**: 1843
11 Otsuka T, Fukunishi N, Sagawa H. Phys. Rev. Lett., 1993, **70**: 1385
12 REN Zhong-Zhou, CHEN Bao-Qiu, MA Zhong-Yu, XU Gong-Ou. Phys. Rev. C, 1996, **53**: R572
13 Brown B A, Hansen P G. Phys. Lett. B, 1996, **381**: 391
14 Zhukov M V, Thompson I J. Phys. Rev. C, 1995, **52**: 3505
15 Iwasaki H, Motobayashi T, Akiyoshi H et al. Phys. Lett. B, 2000, **481**: 7
16 Motobayashi T, Ikeda Y, Ando Y et al. Phys. Lett. B, 1995, **346**: 9
17 Ozawa A, Kobayashi T, Suzuki T et al. Phys. Rev. Lett., 2000, **84**: 5494
18 Stanoiu M, Azaiez F, Dombrádi Zs et al. Phys. Rev. C, 2004, **69**: 034312
19 Suda T, Maruyama K, Tanihata I. RIKEN Accel. Prog. Rep., 2001, **34**: 49
20 Suda T. Proceedings of the International Workshop XXXII on Gross Properties of Nuclei and Nuclear Excitations, Hirschegg, Austria, Edited by M. Buballa, J. Knoll, W. Nörenberg, B.-J. Schaefer, J. Wambach, 2004. 235
21 An international accelerator facility for beams of ions and antiprotons, GSI report, 2002
22 Simon H. Proceedings of the International Workshop XXXII on Gross Properties of Nuclei and Nuclear Excitations, Hirschegg, Austria, Edited by M. Buballa, J. Knoll, W. Nörenberg, B.-J. Schaefer, J. Wambach, 2004, p.290
23 WANG Zai-Jun, REN Zhong-Zhou. Phys. Rev. C, 2004, **70**: 034303
24 Glauber R J. Lectures in Theoretical Physics. New York: Interscience Publishers, 1959. Vol. I.
25 Baker A. Phys. Rev., 1964, **134**: B240
26 Gambhir Y K, Ring P, Thimet A. Ann. Phys. (N.Y.), 1990, **198**: 132
27 Horowitz C J, Serot B D. Nucl. Phys. A, 1981, **368**: 503
28 MA Zhong-Yu, SHI Hua-Lin, CHEN Bao-Qiu. Phys. Rev. C, 1994, **50**: 3170
29 REN Zhong-Zhou, Mittig W, Sarazin F. Nucl. Phys. A, 1999, **652**: 250
30 REN Zhong-Zhou, Mittig W, CHEN Bao-Qiu et al. Phys. Rev. C, 1995, **52**: R20
31 Ring P. Prog. Part. Nucl. Phys., 1996, **37**: 139
32 Warrier L S, Gambhir Y K. Phys. Rev. C, 1994, **49**: 871
33 Tanihata I, Hirata D, Kobayashi T et al. Phys. Lett. B, 1992, **289**: 261
34 Hirata D, Toki H, Tanihata I et al. Phys. Lett. B, 1993, **314**: 168
35 Sharma M M, Nagarajian M A, Ring P. Phys. Lett. B, 1993, **312**: 377
36 Tanihata I, Hirata D, Toki H. Nucl. Phys. A, 1995, **583**: 769
37 Ozawa A, Kobayashi T, Suzuki T et al. Phys. Rev. Lett., 2000, **84**: 5493
38 Audi G, Wapstra A H. Nucl. Phys. A, 1993, **565**: 1
39 De Vries H, De Jager C W, De Vries C. At. Data Nucl. Data Tables, 1987, **36**: 495